A Complex Interplay of Three R2R3 MYB Transcription Factors Determines the Profile of Aliphatic Glucosinolates in Arabidopsis[1][C][W][OA]

Ida Elken Sønderby, Meike Burow, Heather C. Rowe[2], Daniel J. Kliebenstein, and Barbara Ann Halkier*

Plant Biochemistry Laboratory, Villum Kann Rasmussen Research Centre for Pro-Active Plants, and Plant Biochemistry Laboratory, Department of Plant Biology and Biotechnology, Faculty of Life Sciences, Copenhagen University, 1871 Frederiksberg C, Copenhagen, Denmark (I.E.S., M.B., B.A.H.); and Department of Plant Sciences, University of California, Davis, California 95616 (H.C.R., D.J.K.)

While R2R3 MYB transcription factors are a large gene family of transcription factors within plants, comprehensive functional data in planta are still scarce. A model for studying R2R3 MYB control of metabolic networks is the glucosinolates (GLSs), secondary metabolites that control plant resistance against insects and pathogens and carry cancer-preventive properties. Three related members of the R2R3 MYB transcription factor family within Arabidopsis (*Arabidopsis thaliana*), *MYB28*, *MYB29*, and *MYB76*, are the commonly defined regulators of aliphatic GLS biosynthesis. We utilized new genotypes and systems analysis techniques to test the existing regulatory model in which *MYB28* is the dominant regulator, *MYB29* plays a minor rheostat role, and *MYB76* is largely uninvolved. We unequivocally show that *MYB76* is not dependent on *MYB28* and *MYB29* for induction of aliphatic GLSs and that *MYB76* plays a role in determining the spatial distribution of aliphatic GLSs within the leaf, pointing at a potential role of *MYB76* in transport regulation. Transcriptional profiling of knockout mutants revealed that GLS metabolite levels are uncoupled from the level of transcript accumulation for aliphatic GLS biosynthetic genes. This uncoupling of chemotypes from biosynthetic transcripts suggests revising our view of the regulation of GLS metabolism from a simple linear transcription factor-promoter model to a more modular system in which transcription factors cause similar chemotypes via nonoverlapping regulatory patterns. Similar regulatory networks might exist in other secondary pathways.

The number and structural complexity of secondary metabolites evolved in plants are simply mesmerizing (Dixon and Strack, 2003). Secondary metabolites allow the plant to adapt to the ever-changing environment. Ideally, these costly metabolites should be highly adaptable and precisely distributed within the correct tissue at the appropriate time to balance resources utilized in their synthesis with maximal biological impact. Yet, identification and characterization of transcription factors directly controlling secondary metabolite accumulation is still in its infancy (Grotewold, 2008). The direct regulatory network of the glucosinolates (GLSs) encompasses six R2R3 MYB transcription factors from a single gene family within Arabidopsis (*Arabidopsis thaliana*). *ATR1/MYB34*, *MYB51*, and *MYB122* are thought to regulate the Trp-derived (indole) GLS pathway (Celenza et al., 2005; Gigolashvili et al., 2007a; Malitsky et al., 2008), and *MYB28*, *MYB29*, and *MYB76* regulate the Met-derived (aliphatic) GLSs in Arabidopsis accession Columbia (Col-0; Gigolashvili et al., 2007b, 2008; Hirai et al., 2007; Sonderby et al., 2007; Beekwilder et al., 2008; Malitsky et al., 2008). So far, the distinct roles of the R2R3 MYB genes controlling GLS biosynthesis remain largely uncharacterized.

The amino acid-derived GLSs are specific to the order Brassicales and shape plant-pest interactions (Halkier and Gershenzon, 2006; Bednarek et al., 2009). Several advantages make the regulation of aliphatic GLSs an excellent model for the elucidation of regulatory networks (Hirai et al., 2007; Wentzell et al., 2007). First, most genes in the biosynthetic pathway are known (Grubb and Abel, 2006; Halkier and Gershenzon, 2006). The pathway takes place in three stages: a side chain elongation of aliphatic amino acids by incorporation of one to six methylene groups, formation of the core GLS moiety, and finally, secondary modifications of the side chain to generate the plethora of GLS compounds. Second, GLSs can rapidly and reliably be measured, allowing for direct assessment of the connection between homeostasis and induction within

[1] This work was supported by the Villum Kann Rasmussen (VKR) Foundation (grant to VKR Research Centre for Pro-Active Plants to M.B. and B.A.H.), by the National Science Foundation (grant no. DBI 0820580 to D.J.K.), and by the Faculty of Life Sciences of Copenhagen University (Ph.D. stipend to I.E.S.).

[2] Present address: Department of Botany, University of British Columbia, Vancouver, British Columbia, Canada V6T 1Z4.

* Corresponding author; e-mail bah@life.ku.dk.

The author responsible for distribution of materials integral to the findings presented in this article in accordance with the policy described in the Instructions for Authors (www.plantphysiol.org) is: Barbara Ann Halkier (bah@life.ku.dk).

[C] Some figures in this article are displayed in color online but in black and white in the print edition.

[W] The online version of this article contains Web-only data.

[OA] Open Access articles can be viewed online without a subscription.

www.plantphysiol.org/cgi/doi/10.1104/pp.109.149286

numerous conditions and genotypes (Kliebenstein et al., 2001a). Finally, GLSs are present in the model plant Arabidopsis, with all its available genomics tools, and also in important crop plants, where consumption of *Brassica* vegetables has been correlated with a decrease in the occurrence of cancer (Juge et al., 2007; Traka and Mithen, 2009). Therefore, a systematic understanding of GLS regulation can positively affect agriculture and human nutrition as well as our understanding of regulatory networks.

In recent years, *MYB28*, *MYB29*, and *MYB76* have been characterized as direct transcriptional regulators of aliphatic GLS biosynthetic genes after identification using an omics-based methodology (Hirai et al., 2007), a focused transactivation approach (Gigolashvili et al., 2007b, 2008), and a quantitative systems biology approach (Sonderby et al., 2007). The analysis of plants overexpressing *MYB*s in wild-type Col-0 and the transactivation potential of the genes toward GLS biosynthetic genes indicate that the three transcription factors carry largely the same functions (Fig. 1A). However, metabolite analysis of single knockouts revealed that the similar potential shown in the overexpression lines does not fully match the in planta activity. T-DNA mutants in *MYB29* and *MYB76* are decreased in short-chained aliphatic GLSs (one to three cycles of chain elongation; Sonderby et al., 2007; Beekwilder et al., 2008; Gigolashvili et al., 2008), as are T-DNA mutants in *MYB28* that, in addition, are almost devoid of long-chained aliphatic GLSs (four to six cycles of chain elongation; Hirai et al., 2007; Sonderby et al., 2007; Beekwilder et al., 2008). Based on these data, an in planta model might regard all three proteins to act as direct biosynthetic transcriptional activators, with *MYB28* as the major regulator of aliphatic GLSs followed by *MYB29* and *MYB76* having minor, accessory roles (Fig. 1B; Gigolashvili et al., 2009a). However, a double knockout in *MYB28* and *MYB29* is almost devoid of aliphatic GLSs, which suggests an epistatic effect that requires an interacting regulatory mechanism between the two genes (Sonderby et al., 2007; Beekwilder et al., 2008). Furthermore, changes can occur in the relative amounts of individual GLSs, most obviously shown by the change of GLS profiles throughout the development of the plant (Brown et al., 2003). In addition, feeding of aphids only increased short-chained aliphatic GLSs, whereas feeding of the lepidopteran *Spodoptera exigua* increased both short and long-chained aliphatic GLSs (Mewis et al., 2006). Thus, there must be mechanisms by which relative amounts of individual GLSs can be adjusted beyond the link of *MYB28* to long-chained aliphatic GLSs.

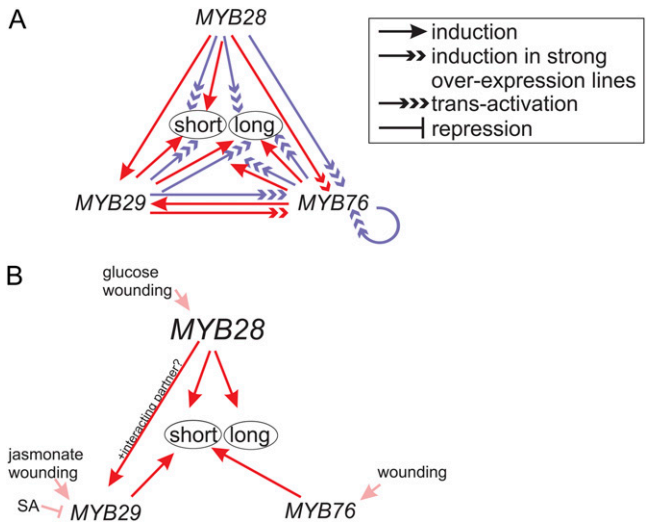

Figure 1. Previous models for the role of *MYB28*, *MYB29*, and *MYB76* in the regulation of aliphatic GLSs in Arabidopsis (accession Col-0) from Hirai et al. (2007), Gigolashvili et al. (2007b, 2008), Sonderby et al. (2007), Beekwilder et al. (2008), and Malitsky et al. (2008). A, Model for potential activities of *MYB28*, *MYB29*, and *MYB76* based on data from overexpression lines and transactivation assays. B, Model for actual regulation in planta. Circles represent short- or long-chained aliphatic GLSs. Lines leading to circles indicate increasing (single arrowheads) effect on metabolites. Lines to genes represent induction of the genes in moderate overexpression lines or in planta regulation (red single arrowheads), strong overexpression lines (red double arrowheads), various treatments in wild-type Col-0 (pink single arrowheads), or transactivation (purple triple arrowheads). In the case of transactivation, arrows pointing toward circles represent activation of biosynthetic genes directing the production of short-chained (*MAM1* and *CYP79F1*) or long-chained (*MAM3* and *CYP79F2*) aliphatic GLSs. The pink T-line represents repression by salicylic acid (SA). [See online article for color version of this figure.]

The general model of flavonoid biosynthesis regulation is that the level of biosynthetic transcripts mirrors the level of accumulating metabolites (Quattrochio et al., 2006). By contrast, recent data indicate that a similar linear correlation is not always present for GLSs. For instance, IQ-DOMAIN1 (IQD1), a calmodulin-binding transcription factor, modifies GLS accumulation and is generally thought to integrate signals when the plant is under biotic stress. Curiously, however, while aliphatic GLS levels are increased in the *iqd1* mutant, a concurrent decrease in the transcript levels of the aliphatic biosynthetic genes *CYP79F1*, *CYP79F2*, and *UGT74B1* is observed (Levy et al., 2005). This contrasts with the coordinated regulation of GLSs metabolites and transcripts by SULFUR LIMITATION1 in response to sulfur deficiency (Hirai et al., 2005; Maruyama-Nakashita et al., 2006; Falk et al., 2007). Moreover, the distribution of GLSs within the leaf (Shroff et al., 2008) cannot be explained by the expression pattern of *MYB28*, *MYB29*, and *MYB76* as shown by promoter-GUS analyses (Gigolashvili et al., 2007b, 2008; Malitsky et al., 2008). This is unlike how the spatial expression pattern of three R2R3 MYB transcription factors specifically directs the accumulation of flavonols (Stracke et al., 2007). Assuming that the MYBs directly control transcript levels of biosynthetic genes in planta, which, in turn, directly reflects the secondary metabolite accumulation, this does not seem applicable to GLS biosynthesis.

The indications for a complex regulatory hierarchy within aliphatic GLS regulation prompted us to investigate the individual roles of *MYB28*, *MYB29*, and *MYB76* in planta and their potential interactions to unravel their roles in shaping the GLS profile of the plant. We show that *MYB29* does not affect transcript levels for any of the biosynthetic genes, while *MYB28* constitutes the major transcriptional inducer. The combination of transcriptional analysis with GLS profiles of the knockouts revealed an intriguing uncoupling of the level of biosynthetic transcripts from the level of aliphatic GLSs, since similar levels of biosynthetic transcript resulted in surprisingly different chemotypes. We unequivocally demonstrate that *MYB76* has a *MYB28*- and *MYB29*-independent role in Arabidopsis (accession Col-0) and that *MYB76* has transcriptional effects on specific parts of the biosynthetic pathway. Finally, altered aliphatic GLS distribution in the leaves in different *myb* knockouts and overexpressors indicates that the spatial expression pattern of *MYB76* in particular determines the pattern of aliphatic GLS accumulation. These data prompted us to suggest an improved model for the regulation of aliphatic GLSs.

RESULTS

MYB76 Is Independent of *MYB28* or *MYB29* for Induction of Aliphatic GLS Biosynthesis

Due to no significant impact (Gigolashvili et al., 2008) or only a small change (Sonderby et al., 2007) on GLS levels in *myb76* knockdowns, *MYB76* has been concluded to carry out a minor, possibly accessory role in aliphatic GLS biosynthesis within the Col-0 accession (Gigolashvili et al., 2009a). Combined with the minute aliphatic GLSs measured in the *myb28 myb29* double knockout (Sonderby et al., 2007; Beekwilder et al., 2008), this led us to hypothesize that *MYB76* might require *MYB28* and *MYB29* to induce GLS biosynthesis in planta. To test this hypothesis, we overexpressed *MYB76* in the *myb28-1 myb29-1* double knockout background by way of the cauliflower mosaic virus 35S promoter, allowing a direct test of the capability of *MYB76* to induce aliphatic GLSs in the absence of both *MYB28* and *MYB29*.

Foliar aliphatic GLSs were detected in independent T1 transformants. Contrary to the sole impact on short-chained aliphatic GLS in the *myb76* knockdown mutants, both short-chained and long-chained aliphatic GLSs were induced up to 50% and 60% of wild-type Col-0, respectively. Both methylthioalkyl- and methylsulfinylalkyl-GLSs were produced (for GLS abbreviations, see Supplemental Table S1), thereby indicating that *MYB76* can induce both core biosynthesis and the secondary modification pathway encompassing FMO_{GSOX}s, which convert methylthioalkyl- to methylsulfinylalkyl-GLSs (Hansen et al., 2007; Li et al., 2008; Supplemental Tables S2 and S3). Analysis of T2 leaves indicated transgene silencing, since the plants only contained 5% short-chained aliphatic GLSs in comparison with the wild type and undetectable levels of long-chained aliphatic GLSs (data not shown). Similarly, we have observed the loss of chemotype in subsequent generations when overexpressing *MYB76* in the wild-type Col-0 background (data not shown).

Previous overexpression analysis showed that *MYB76* had the potential to regulate aliphatic seed GLS levels in Arabidopsis Col-0 plants (Sonderby et al., 2007). These experiments, however, did not address if *MYB76* requires a functional *MYB28* and/or *MYB29* to induce GLSs in seeds. In T2 seeds of the *myb28-1 myb29-1* knockout plants overexpressing *MYB76*, the different lines had short-chained aliphatic levels of up to 140% and long-chained aliphatic GLSs of 10% to 30% of the levels in wild-type Col-0 (Fig. 2; Supplemental Tables S4 and S5). While short-chained methylthioalkyl- and methylsulfinylalkyl-GLSs accumulated to levels above the wild type, the short-chained seed-specific GLSs, 3bzop and 4bzob, did not exceed wild-type levels.

In summary, these data show that *MYB76* can function independently of *MYB28* and *MYB29* in controlling both short-chained and long-chained aliphatic GLSs in leaves as well as in seeds. Furthermore, *MYB76* can induce long-chained aliphatic GLSs, an ability previously solely ascribed to the regulatory realm of *MYB28*.

myb28-1 myb76 Double Knockouts Show Independence of *MYB76* from *MYB28*

Since *myb76* and *myb29* single knockout mutants both show decreases only in short-chained aliphatic GLSs (Sonderby et al., 2007; Beekwilder et al., 2008; Gigolashvili et al., 2008) and *MYB29* and *MYB76* are tandemly duplicated genes, the two genes might functionally overlap in planta. To explore the role of *MYB76* and a possible genetic interaction of *MYB76* with *MYB28* (as shown for *MYB28* and *MYB29*; Sonderby et al., 2007; Beekwilder et al., 2008), we investigated the GLS profile of homozygous *myb28-1 myb76* knockouts as well as wild-type Col-0, *myb76*, and *myb28-1* obtained from crossing *myb28-1* with either *myb76-1* or *myb76-2* (Fig. 3). An ANOVA of GLS levels between *myb76-1* and *myb76-2* as well as between *myb28-1 myb76-1* and *myb28-1 myb76-2* showed no significant difference between the two *myb76* lines, allowing us to combine the lines to test the effect of the absence of *MYB76* rather than the effect of one specific insertion allele versus the wild type (Supplemental Table S6).

The *myb28-1 myb76* double knockouts retained 33% of the short-chained foliar aliphatic GLSs in comparison with wild-type Col-0. Thereby, the *myb28-1 myb76* foliar aliphatic GLS phenotype is an additive combination of the two single mutants (Fig. 3; Supplemental Table S7), which is in contrast to the emergent quality

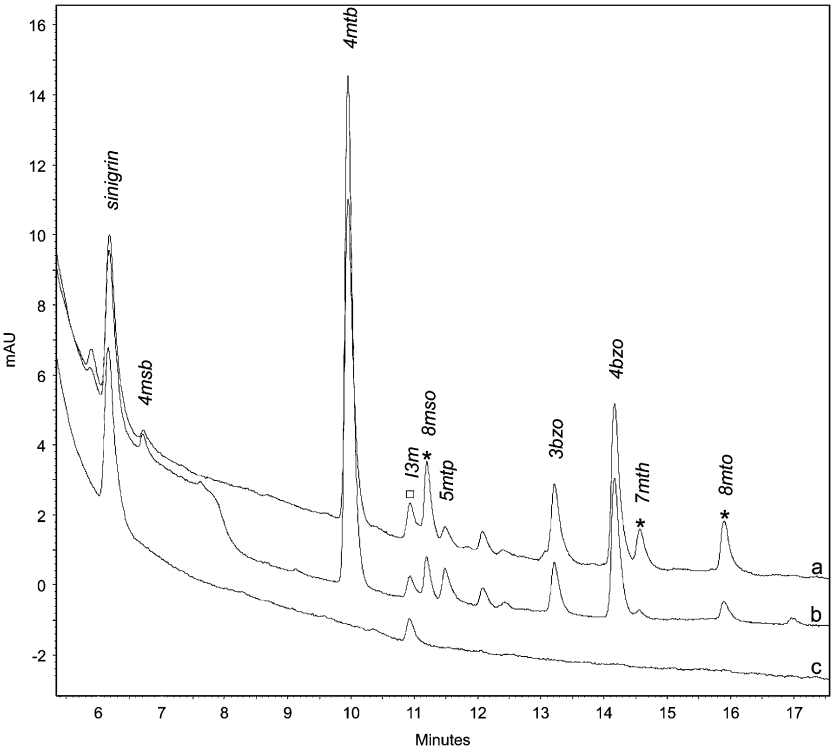

Figure 2. HPLC analysis of GLSs in seeds of wild-type Col-0 (trace a), T2 seeds of a plant overexpressing *MYB76* in the *myb28-1 myb29-1* double knockout background (trace b), and seeds of *myb28-1 myb29-1* double knockout (trace c). GLSs were extracted from 10 seeds using 6 nmol of sinigrin as an internal standard and analyzed as desulfoglucosinolates by HPLC (for details, see "Materials and Methods"). Peaks representing individual compounds are denoted using the abbreviations in Supplemental Table S1. Long-chained aliphatic GLSs are marked by asterisks and indole GLSs by squares. For quantitative results and more lines, see Supplemental Table S4. mAU, Milli absorption units.

observed in the almost aliphatic GLS-free *myb28 myb29* double knockout mutant (Sonderby et al., 2007; Beekwilder et al., 2008). The decrease in the *myb28-1 myb76* knockout in comparison with the single mutants was observed for all short-chained aliphatic GLSs (i.e. 3msp, 4mtb, 4msb, and 5msp; Supplemental Table S1). The only nonadditive interaction effect observed in the aliphatic GLS data was for 4mtb (Supplemental Table S6), suggesting an epistatic interaction of *MYB28* and *MYB76* upon the *FMO*s that convert methylthioalkyl- to methylsulfinylalkyl-GLSs. In addition, an epistatic effect for total indole GLS levels was observed in the data set (Supplemental Table S6). The analysis of homozygous F2 progeny was identical to the F3 generation presented here (data not shown).

Seeds are one of the predominant sites for the accumulation for aliphatic GLSs with a unique GLS profile (Brown et al., 2003). No significant difference was found in seed GLS between the *myb28-1* and *myb28-1 myb76* knockout mutants (Table I; Supplemental Table S8). Since the *myb76* single knockdowns do not have a seed GLS chemotype (Table I; Supplemental Table S8), these data again support the absence of an epistatic effect between *MYB28* and *MYB76* for the vast majority of GLSs. In conclusion, the *myb28-1 myb76* knockout mutant data provide additional support that *MYB76* has regulatory capabilities on its own.

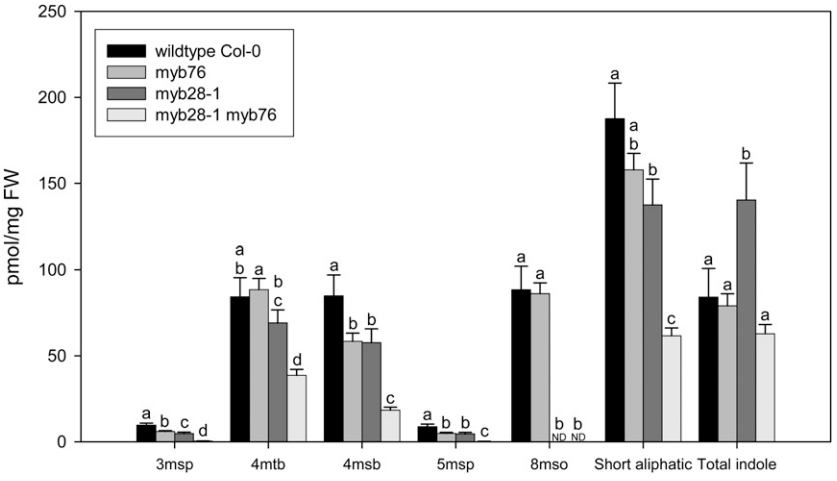

Figure 3. Comparison of foliar GLS levels in wild-type Col-0, *myb76*, *myb28-1*, and *myb28-1 myb76* knockouts. GLSs were extracted from 30 to 70 mg of leaf material derived from 21- to 24-d-old plants and quantified as desulfoglucosinolates by HPLC. $n = 11$ for wild-type Col-0, $n = 32$ for *myb76*, $n = 25$ for *myb28-1*, and $n = 56$ for *myb28-1 myb76*. The data are sums of two independent experiments and were analyzed via ANOVA (Supplemental Table S6). Individual indole GLSs can be found in Supplemental Table S1. Different letters indicate significant differences at $P < 0.05$. FW, Fresh weight; ND, not detected.

Table I. *Seed GLSs in wild-type Col-0, myb28-1, myb76, and myb28-1 myb76 T-DNA knockouts*

Mean shows the average GLS content in pmol per 10 seeds using the abbreviations in Supplemental Table S1. SE is the standard error for the line. These data represent two independent biological replicates. *n* is the number of replicates per genotype. The data for the two *myb76* alleles and the two *myb28-1 myb76* alleles were pooled, as there was no significant difference in the GLS phenotype between the different alleles (Supplemental Table S8). Different letters (a, b, c) represent significant differences at $P < 0.05$ between wild-type Col-0 and the homozygous mutant lines as determined by ANOVA (Supplemental Table S8).

GLS	Wild-Type Col-0 (*n* = 8)		*myb76* (*n* = 15)		*myb28-1* (*n* = 8)		*myb28-1 myb76* (*n* = 15)	
	Mean	SE	Mean	SE	Mean	SE	Mean	SE
3bzop	0.57a	0.03	0.56a	0.04	0.31b	0.03	0.31b	0.01
4mtb	3.98a	0.16	3.28a	0.21	1.48b	0.16	1.17b	0.10
4msb	0.23a	0.04	0.32a	0.04	0.28a	0.06	0.33a	0.08
4bzob	0.80a	0.06	1.17ab	0.11	0.99b	0.09	0.89a	0.07
5mtp	0.15a	0.01	0.11a	0.01	0.07b	0.01	0.05c	0.01
7mth	0.88a	0.08	0.75a	0.09	0.01b	0.00	0.01b	0.00
8mto	1.62a	0.10	1.51a	0.16	0.02b	0.00	0.01b	0.00
8mso	1.30a	0.10	1.41a	0.09	0.02b	0.01	0.02b	0.01
Short	5.73a	0.16	5.44a	0.34	3.13b	0.27	2.76b	0.16
Long	3.80a	0.23	3.66a	0.31	0.05b	0.01	0.05b	0.01
Total	9.53a	0.31	9.10a	0.60	3.18b	0.27	2.81b	0.16
I3M	0.08a	0.01	0.07b	0.01	0.07b	0.01	0.11b	0.01

MYB29 Alone Can Induce Long-Chained Aliphatic GLSs

MYB28 knockout mutants are strongly reduced in or lack detectable long-chained aliphatic GLSs, indicating *MYB28* as the sole regulatory factor for these GLSs. However, the above experiments showed that *MYB76* could induce long-chained aliphatic GLSs in the absence of both *MYB28* and *MYB29* (Fig. 2). Possibly, *MYB29* could likewise induce long-chained aliphatic GLSs in the absence of *MYB28* and *MYB76* in spite of its pure short-chained aliphatic GLS knockout mutant chemotype. To test this, we overexpressed *MYB29* in the *myb28-1 myb76* double knockout background. Ten independent T1 transformants were generated, all of which showed the production of long-chained aliphatic GLSs, as was likewise observed in both the T2 seeds and their progeny (Fig. 4; Supplemental Tables S2–S4; data not shown). Thus, *MYB29* can control the biosynthesis of these compounds independently of *MYB28* and *MYB76*. Interestingly, the short-chained aliphatic GLSs were elevated in comparison with both *myb28-1 myb76* and wild-type Col-0 in both leaves (Supplemental Tables S2 and S3) and seeds (Supplemental Tables S4 and S5). In seeds, the increase in short-chained GLSs was far more pronounced than the increase in long-chained GLSs. This suggests that while MYB29 can induce long-chained aliphatic GLSs, *MYB28* may still be necessary for optimal long-chained aliphatic GLS accumulation in seeds.

Genome-Wide Transcriptional Analysis of T-DNA Knockouts Points to Divergent Roles of *MYB28*, *MYB29*, and *MYB76* in Planta

Individual overexpression of *MYB28*, *MYB29*, and *MYB76* revealed both altered GLS accumulation (Gigolashvili et al., 2007b, 2008; Hirai et al., 2007; Sonderby et al., 2007; Malitsky et al., 2008) and a significant overlap in GLS transcripts induced by the three *MYB* genes (Sonderby et al., 2007). Thus, the regulatory model based on overexpression lines and transactivation data (Fig. 1A) suggests a transcriptional analysis of the single knockouts to identify similar regulatory modules for the three MYBs. However, the different additive and epistatic genetic effects observed in the GLS profiles of T-DNA double knockouts suggest a much more complex pattern in planta, with some overlap in regulatory modules but also extensive specificity. To test the transcriptional regulatory capabilities of *MYB28*, *MYB29*, and *MYB76*, we performed Affymetrix ATH1 GeneChip microarrays on the following knockouts: *myb28-1*, *myb29-1*, *myb29-2*, *myb76-1*, *myb76-2*, and *myb28-1 myb29-1*. GLS analysis confirmed the expected chemotypes of all plants used for RNA extraction (data not shown).

As multiple alleles of both *MYB29* and *MYB76* were included in the analysis, we utilized independent ANOVAs to test whether the difference in each transcript was significantly different between each mutant allele compared with the wild type (Supplemental Table S10). ANOVA of transcript levels suggested that *myb76-1* and *myb76-2* (Supplemental Table S10) were identical, allowing us to combine the means of the two lines and test the effect of lack of *MYB76* rather than the effect of any single insertion allele versus the wild type. In contrast, *myb29-1* and *myb29-2* occasionally showed opposite effects on genes, and the ANOVA showed that the effect on gene expression of the two alleles was significantly different. As such, although no difference was found in the effect on the GLS biosynthetic genes between the two knockouts, we did not combine the data and focused on the transcript data from the *myb29-2* mutant, as the *myb29-1* allele did not show a significantly lower transcript of *MYB29*

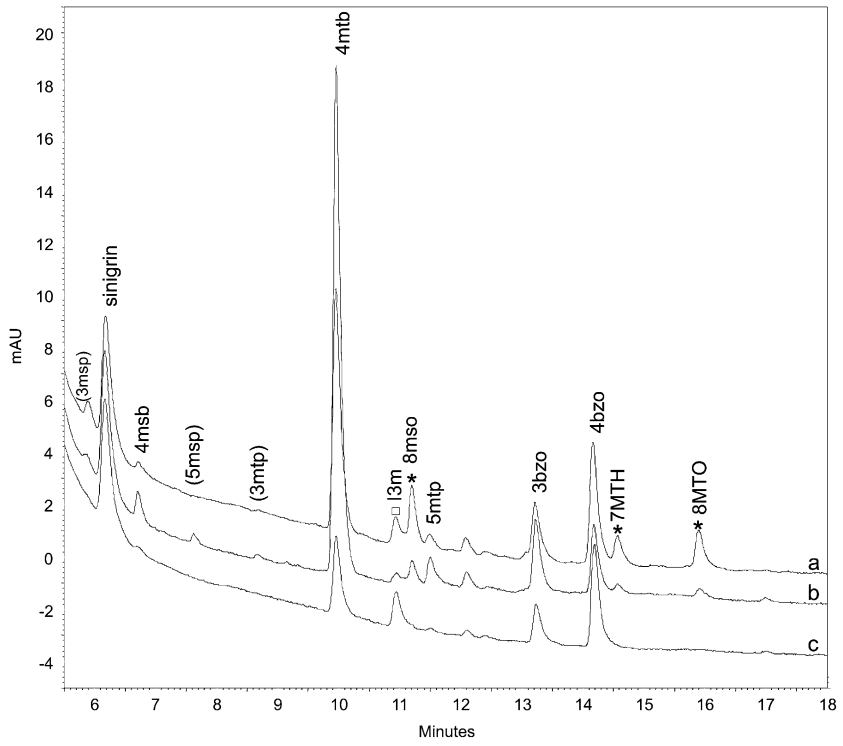

Figure 4. HPLC analysis of GLSs in seeds of wild-type Col-0 (trace a), T2 seeds of a plant overexpressing *MYB29* in the *myb28-1 myb76-2* double knockout background (trace b), and seeds of *myb28-1 myb76-2* double knockout (trace c). GLSs were extracted from 10 seeds using 6 nmol of sinigrin as an internal standard and analyzed as desulfoglucosinolates by HPLC (for details, see "Materials and Methods"). Compounds are denoted using the abbreviations in Supplemental Table S1. Long-chained aliphatic GLSs are marked by asterisks and indole GLSs by squares. For quantitative results and more lines, see Supplemental Table S4. mAU, Milli absorption units.

in comparison with wild-type Col-0 (Table II; Supplemental Table S9).

Using a false discovery rate (FDR) of 0.05, *myb76* had the smallest number of changed transcript levels in comparison with Col-0 with 668 altered transcripts (394 down, 262 up), followed by *myb28-1* with 1,066 altered transcripts (584 down, 449 up), *myb28-1 myb29-1* with 1,412 altered transcripts (666 down, 726 up), and finally *myb29-2* with 2,914 altered transcripts (1,115 down, 1,799 up; Supplemental Table S10). This is a rather large number of altered transcripts, but the experimental design likely allowed us to identify both direct and indirect targets. Given the centrality of GLSs to Arabidopsis defense, such a number of direct and indirect links might be expected. Additionally, GLSs have recently been shown to influence stomatal closure via the abscisic acid pathway (Zhao et al., 2008), which indicates that we are just beginning to understand their linkages to the rest of the genome. A Venn diagram of the three single gene knockouts, *myb28-1*, *myb29-2*, and *myb76*, revealed that the overlap between the three mutants was indistinguishable from random (Fig. 5A; χ^2, $P = 0.687$). This shows that the three genes have distinct transcriptional roles in planta. Of the five genes showing expression overlap among all three single *myb* knockouts, only one had any apparent link to the GLS pathway. *SULTR2;1* (*At5g10180*), a low-affinity sulfate transporter, was significantly decreased in all genotypes. The other four genes were *GASA5* (*At3g02885*), *FAS1* (*At1g65470*), a glycosylphosphatidylinositol transamidase component family protein (*At5g19130*), and an F-box protein (*At5g03970*) with no known function linked to GLS biosynthesis.

MYB28 Is the Key Transcriptional Activator of Aliphatic Biosynthetic Transcripts

Having established that the different *myb* single knockouts conferred different transcriptional effects at the overall level, we more deeply queried the distinct roles of *MYB28*, *MYB29*, and *MYB76*.

MYB28 transcript was nearly absent in the *myb28-1* knockout (Table II; Fig. 6). Analysis of *myb28-1* versus the wild type showed that 13 out of 28 transcripts of known or putative aliphatic GLS biosynthetic genes were significantly lowered (Fig. 6; Table II). Interestingly, the largest fold changes were centered on the chain-elongation machinery, *BCAT4*, *MAM1*, *MAM3*, the *IPMI*s, and *BAT5*, a transporter putatively involved in the chain elongation pathway (Gigolashvili et al., 2009b; Sawada et al., 2009). Additionally, large impacts on late genes in the pathway were present, as shown by down-regulation of FMO_{GSOX1} and FMO_{GSOX3}. However, the general effect on the rest of the core biosynthesis and secondary modification enzymes was more modest, thereby still upholding some basic transcriptional level of the pathway (Table II). Interestingly, *MYB29* was decreased 43% in the *myb28-1* mutant. While this was not statistically significant in this experiment, it is in accordance with a previously observed significant down-regulation of *MYB29* in a different *myb28* knockout mutant, as measured by quantitative reverse transcription (RT)-PCR (Beekwilder et al., 2008).

These data point to a key importance of *MYB28* for transcriptional regulation of the side chain elongation component of the aliphatic GLS biosynthetic enzymes.

Table II. *Transcriptional effects on aliphatic GLS genes in various myb knockouts*

The FDR adjusted *P* values (FDR = 0.05) and mutant effects for the known or predicted GLS genes were extracted from Supplemental Table S9. For indole GLS regulators and biosynthetic genes, see Supplemental Table S10. NS, Not significant.

Gene	*P* for Wild Type Versus					(Mutant − Wild Type)/Wild Type				
	myb28-1 myb29-1	*myb28-1*	*myb29-1*	*myb29-2*	*myb76*	*myb28-1 myb29-1*	*myb28-1*	*myb29-1*	*myb29-2*	*myb76*
						%				
Confirmed genes in aliphatic GLS biosynthesis										
BCAT3	NS	0.000	NS	NS	NS	−17	−19	10	5	−4
BCAT4	0.000	0.000	NS	NS	NS	−96	−94	−20	6	−15
MAM1	0.000	0.014	NS	NS	NS	−97	−95	−7	30	−7
MAM3	0.000	0.002	NS	NS	NS	−88	−90	38	0	0
CYP79F1	NS	0.033	NS	NS	NS	−33	−36	−14	−4	−16
CYP83A1	0.000	0.019	NS	NS	NS	−91	−88	−5	36	−5
C-S LYASE	0.006	NS	NS	NS	NS	−30	−23	−2	3	−8
UGT74B1	NS	NS	NS	NS	NS	−13	8	8	21	−20
SOT18	0.015	NS	NS	0.016	NS	−44	−39	−5	50	−9
SOT17	NS	NS	NS	NS	0.027	−39	−6	7	−1	−22
FMO_{GSOX1}	0.000	0.031	NS	NS	0.019	−83	−76	−18	4	−32
FMO_{GSOX2}	NS	NS	NS	NS	NS	−11	−18	−6	8	−1
FMO_{GSOX3}	0.005	0.013	NS	NS	NS	−80	−77	−33	29	−5
FMO_{GSOX4}	0.043	NS	NS	NS	NS	47	8	21	10	−7
FMO_{GSOX5}	NS	NS	NS	NS	NS	8	−5	−5	−8	−2
AOP3	NS	NS	NS	NS	NS	−1	3	12	5	−6
AOP2	NS	NS	NS	NS	0.028	−54	−52	−49	−3	−23
GS-OH	NS	NS	NS	NS	NS	−7	3	23	−2	−12
BZO1	NS	NS	NS	NS	NS	0	4	−2	5	−3
Myb28	0.000	0.001	NS	0.041	NS	−94	−95	−14	35	0
Myb29	0.008	NS	NS	0.008	0.001	−57	−43	−28	−35	−42
Myb76	NS	NS	NS	NS	NS	−14	−14	−3	3	−7
Genes putatively involved in aliphatic GLS biosynthesis/intermediate transport										
IPMI LSU1	0.013	NS	NS	NS	NS	−13	−9	7	−3	−3
IPMI SSU2	0.000	0.001	NS	NS	NS	−81	−80	−5	17	−10
IPMI SSU3	0.001	0.002	NS	NS	NS	−81	−78	−41	60	−6
IMD3	0.010	NS	NS	NS	NS	−43	−42	15	4	−10
BAT5	0.001	0.015	NS	NS	NS	−77	−72	−17	20	−17
ATGSTF11	0.006	0.047	0.049	NS	NS	−52	−50	−33	50	−8
ATGSTF9	0.016	NS	NS	NS	NS	−32	−23	−17	3	−3
ATGSTU20	0.001	NS	NS	NS	NS	−68	−62	−12	12	−15
UGT74C1	NS	0.010	NS	NS	NS	−21	−31	−6	20	1

Additionally, it shows an intriguing capacity within GLS regulation: even very low expression levels of parts of the GLS biosynthetic apparatus can maintain two-thirds of the wild-type levels of short-chained aliphatic GLS in the *myb28-1* mutant (Fig. 3), thereby hinting at an uncoupling of biosynthetic transcripts from GLS chemotypes.

myb29 Is Not Affected in the Transcription of Aliphatic Biosynthetic Genes

As *MYB29* has been described as the second most important aliphatic GLS regulator, we next investigated the transcript differences between wild-type Col-0 and *myb29-2*. Transcript of *MYB29* was only 35% decreased in the *myb29-2* single knockout (Table II; Fig. 6). However, since previous RT-PCR in the important R2R3 MYB binding domain did not detect transcript in the *myb29-2* mutant (Sonderby et al., 2007) and the ATH1 probes are situated farther downstream in the gene, we regard the discrepancy to be caused by aberrant downstream transcript and thus *myb29-2* as a true functional knockout. This is supported by its aliphatic GLS chemotype. To our surprise, however, a direct comparison of transcript levels between the *myb29-2* knockout and the wild type did not show any decrease in transcript abundance for genes within the aliphatic biosynthetic pathway (Figs. 5C and 6). The *myb29-1* mutant also did not alter the accumulation of aliphatic GLS gene transcripts (Table II). On the contrary, there was a tendency for the biosynthetic transcript levels to be elevated, most prominently shown in *myb29-2* by a significant increase of 50% in the transcript of *SOT18*, one of the sulfotransferases in core GLS biosynthesis (Table II; Fig. 6).

At first glance, these data seem to contradict previous understanding of *MYB29* as a positive transcriptional activator of aliphatic biosynthetic transcripts. A potential explanation for this discrepancy may come from a significant increase in *MYB28* transcript in the *myb29-2* knockout, which may lead to the wild-type transcript levels of the other GLS genes (Table II; Fig.

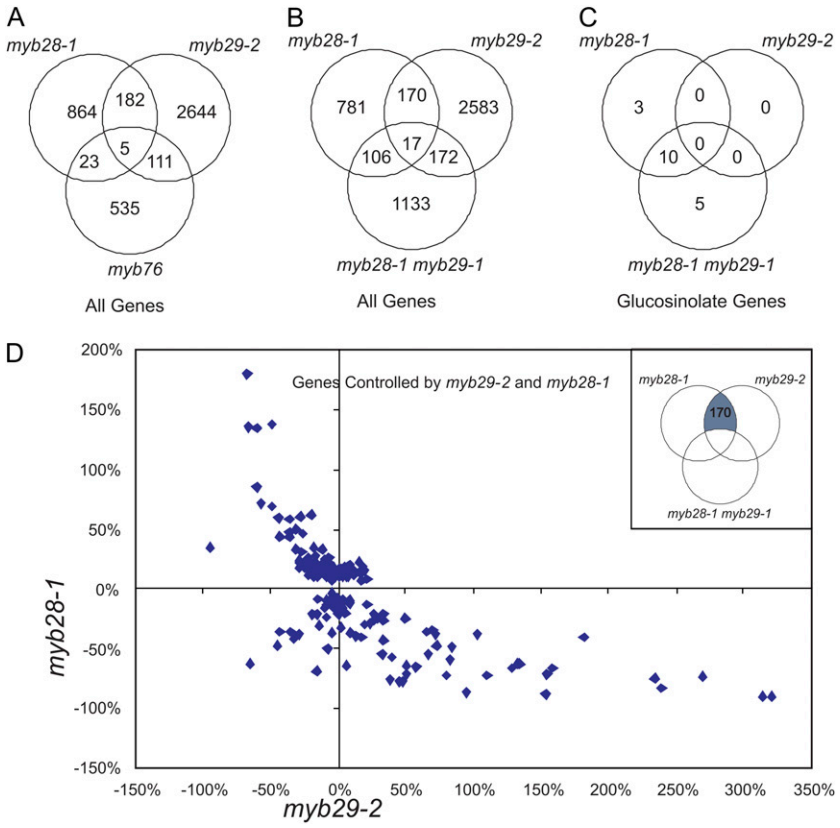

Figure 5. Overlap of genes altered in gene expression levels among different *myb* knockout mutants. A to C, Venn diagrams in which each ring of the individual Venn diagram shows the number of genes present on the ATH1 array whose transcript level was statistically significantly altered as compared with the wild type by the given knockout mutation. Statistical significance was determined by individual gene ANOVAs using a FDR of 0.05 (Supplemental Table S10). A, Overlapping genes in the *myb28-1*, *myb29-2*, and *myb76* single knockouts as compared with wild-type Col-0. B, Overlapping genes in the *myb28-1*, *myb29-2*, and *myb28-1 myb29-1* knockout mutants as compared with wild-type Col-0. C, As in B, but showing only known and putative GLS genes (Table II). D, Plot of changed transcripts in the *myb28-1* and *myb29-2* single knockouts. The correlation plot was obtained by taking the 170 genes showing differential expression in both the *myb28-1* and *myb29-2* mutant lines but not in the *myb28-1 myb29-1* double knockout (inset and B). These genes identify a negative correlation of effects between the two mutants (slope = -0.24, $r = 0.42$, $P < 0.0001$, $n = 170$). [See online article for color version of this figure.]

6). This suggests a compensatory up-regulation of *MYB28* in the absence of *MYB29*, leading to elevated transcript abundance. However, this does not explain the lower short-chained aliphatic GLS chemotype of *myb29-2*.

The *myb28-1 myb29-1* Double Knockout Shows a Similar Uncoupling of Biosynthetic Transcripts from Chemotypes as *myb28-1*

The almost aliphatic GLS-free chemotype of the *myb28-1 myb29-1* mutant suggests a corresponding abolition of aliphatic biosynthetic transcripts in the mutant. Indeed, the absence of *MYB28* and *MYB29* in the double knockout did lead to a broad decrease in transcript abundance for all the aliphatic GLS biosynthetic phases: chain elongation, core biosynthesis, and secondary modification. Sixteen of the 28 transcripts of known or putative aliphatic GLS biosynthetic genes were significantly decreased, as were the transcripts of *MYB28* and *MYB29* themselves (Fig. 6; Table II). Intriguingly, however, even though several genes became significantly down-regulated in the *myb28-1 myb29-1* double knockout in comparison with the *myb28-1* knockout, the observed proportional decrease in biosynthetic transcripts was no lower than that observed in the *myb28-1* knockout (Fig. 6; Table II). Thus, the epistatic effect of *MYB28* and *MYB29* shown at the GLS level is not mirrored as an epistatic effect on the total level of biosynthetic transcripts but only on individual transcripts.

GLS accumulation within a certain tissue is determined by the amount of biosynthesis, catabolism, and transport. Thus, changes in any of the processes might cause the uncoupling. However, no significant differences could be detected in the transcription of genes in the degradation pathways (i.e. the β-glucosidases *TGG1*, *TGG2*, *PEN2*, and *PYK10* as well as the specifier proteins *ESP*, *NSP*s, and *ESM1*) involved or putatively involved in GLS breakdown (Supplemental Table S11). However, myrosinase-binding protein 1 (*MBP1*; *At1g52040*), which has been suggested to serve a function in endogenous turnover of GLSs in *Brassica napus* (Andreasson et al., 2001), was one of the most up-regulated genes in the *myb76* knockdowns (59%) and nonsignificantly up-regulated 63% and 52% in the *myb29-2* and *myb28-1 myb29-1* knockouts, respectively. It still remains unknown what the role of *MBP1* is in plants. However, if the *MYB*s affect breakdown, then *MBP1* or other uncharacterized proteins could account for it.

Previous data have shown large transcriptional effects on sulfur metabolism when overexpressing the three *MYB* genes in the wild-type Col-0 background (Sonderby et al., 2007; Malitsky et al., 2008). Therefore, we queried whether transcripts of the following sulfur utilization pathways were changed in the knockouts: sulfate transport and assimilation, phosphoadenosine-

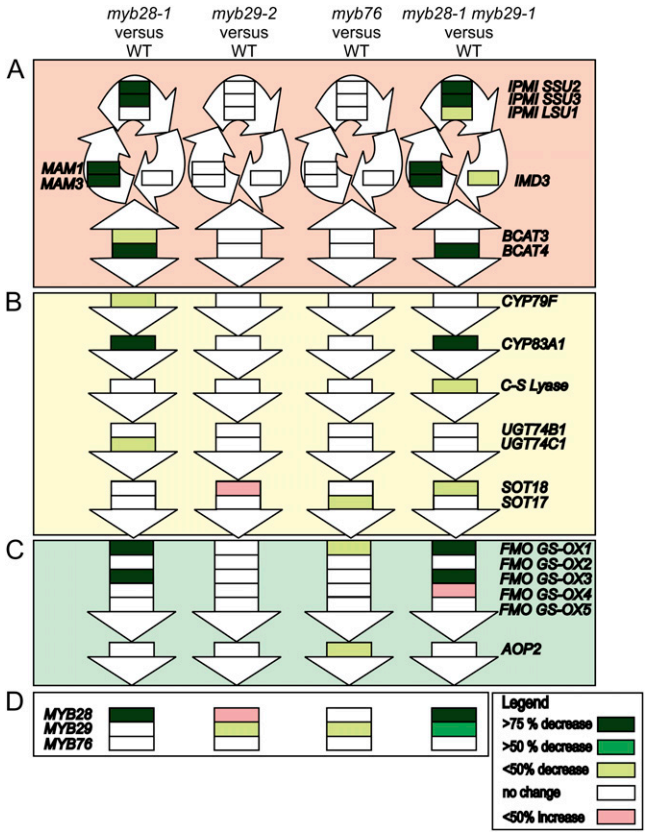

Figure 6. Altered transcript accumulation for GLS biosynthetic genes in different *myb* knockouts. The scheme denotes the GLS biosynthetic pathway, with each arrow representing a biosynthetic step in the pathway and the corresponding gene listed on the side. Boxes in the arrows illustrate changes in transcription levels of the respective biosynthetic gene in the various knockouts, *myb28-1*, *myb29-2*, *myb76*, and *myb28-1 myb29-1*, versus wild-type (WT) Col-0. Green shades represent significant decreases in expression, pink represents significant increases in expression, and white represents no significant change. A, The Met chain-elongation machinery. B, Synthesis of the core methylthioalkyl-GLS structure. C, Secondary modifications of the side chain. D, The *MYB* transcription factors. [See online article for color version of this figure.]

5′-phosphosulfate, Cys, *S*-adenosyl Met and Met production, and homo-Cys conversion. While sulfur utilization was not affected in the *myb28-1* and *myb76* single knockouts, *myb29-2* was up-regulated in a sulfate transporter (SULTR5;1; *At1g80310*) together with three adenosine-5′-phosphate reductases, *APR1* (*At4G04610*), *APR2* (*At1G62180*), and *APR3* (*At4G21990*; Supplemental Table S11) that all reduce adenosine-5′-phosphate to sulfite. In contrast, sulfate assimilation appeared to be down-regulated in the *myb28-1 myb29-1* knockout. *APR1* and *APR3* were down-regulated 75% along with a significant down-regulation of an ATP sulfurylase, *ATPS1* (*At3G22890*), the sulfite reductase, SiR (*At5G04590*), and the sulfate transporters *SULTR1;2* (*At1g78000*), *SULTR2;1* (*At5g10180*), and *SULTR4;2* (*At3g12520*). In opposition, the ATP sulfylase, *ATPS2* (*AT1G19920*), and *SULTR3;1* (*At3g51895*) were significantly up-regulated in the double knockout. In conclusion, the aliphatic GLS MYBs seems to regulate both biosynthetic transcripts and precursor availability, as suggested from data on overexpression lines (Sonderby et al., 2007; Malitsky et al., 2008).

Hitherto, all data support a role for the *MYB*s as exclusively positive regulators of aliphatic GLS genes. However, FMO_{GSOX4}, one of the sulfur-oxygenating enzymes in the secondary modification of GLSs (Li et al., 2008), was up-regulated in the *myb28-1 myb29-1* double knockout but was not affected in any of the single knockouts (Fig. 6). This suggests that *MYB28* and *MYB29* in concert can function as negative regulators. To test if *MYB28* and *MYB29* can have unexpected combinatorial roles with unidentified genes, we generated a Venn diagram illustrating overlap in altered transcript levels between *myb28-1*, *myb29-2*, and *myb28-1 myb29-1* (Fig. 5, B and C). A total of 170 genes were significantly changed in both *myb28-1* and *myb29-2* but not in the *myb28-1 myb29-1* knockout (Fig. 5B). This represents genes whose significance disappears in *myb28-1 myb29-1*. When the changes in transcript levels of the 170 genes were plotted against each other, the correlation plot gave a negative slope (Fig. 5D). This suggests that *MYB28* and *MYB29* have opposing effects on most genes in this category, such that the *myb28* knockout represses a gene that the *myb29* knockout activates and vice versa. This antagonistic functionality could explain why the wild type and the *myb28-1 myb29-1* double knockout have similar levels of these transcripts. In fact, only a few of these genes appear to be positively regulated by both *MYB28* and *MYB29*.

Accordingly, *MYB28* and *MYB29* can act as both activators and repressors with a significant level of independence. The repressor effect is particularly conspicuous in the case of *MYB29*, since approximately two-thirds of the genes significantly changed in the *myb29* knockout are up-regulated genes (Supplemental Table S10). It remains to be seen if these are direct or indirect targets of MYB29.

MYB76 Controls Secondary Modification Enzymes and *MYB29*

Analysis of the microarray data for the *myb76* mutants did not show a significant down-regulation of *MYB76* transcript (Fig. 6; Table II), which is already very lowly abundant in the wild type. However, previous RT-PCR analysis of the *myb76* knockdowns showed considerably reduced *MYB76* transcript (Sonderby et al., 2007). In accordance with the modest 30% decrease in short-chained aliphatic GLSs (Fig. 3), the *myb76* knockdown alleles were only affected in three aliphatic biosynthetic transcripts: two in the secondary modification pathway, FMO_{GSOX1} and *AOP2* (the protein is nonfunctional in the Col-0 accession but the gene is nevertheless transcribed; Kliebenstein et al.,

2001b), and the sulfotransferase *SOT17* in core biosynthesis (Fig. 6; Table II). These data agree with the *myb76* knockdown having its largest effect on methylsulfinylated short-chained aliphatic GLSs (Fig. 3), which are predominantly sulfur oxygenated by FMO_{GSOX1} in the leaves (Hansen et al., 2007). Interestingly, *MYB29* transcript was significantly decreased in both *myb76* knockdowns, suggesting that part of the effect in the *myb76* knockdowns might be conferred through decreased expression of *MYB29*.

Altogether, the microarray data draw a picture of an interdependency of the three *MYB* genes, with each gene controlling its independent module to uphold GLS biosynthesis. Furthermore, the data reveal that the transcriptional level of biosynthetic genes does not fully reflect the level of aliphatic GLSs in the plant.

Knockout Mutants of *MYB28*, *MYB29*, and *MYB76* Show Altered Distribution of Aliphatic GLSs within the Leaf

Results based on dissection and ion intensity maps from matrix-assisted laser-desorption ionization time of flight of leaves have shown that GLSs are particularly abundant in the edge and midvein (Shroff et al., 2008). The abundance of GLSs in the edge is in contrast to the expression patterns obtained by promoter-GUS fusions of genes from chain elongation, core biosynthesis, and aliphatic regulation genes, which all indicate that biosynthesis takes place in and around the veins of leaves (Reintanz et al., 2001; Chen et al., 2003; Grubb et al., 2004; Schuster and Binder 2005; Gigolashvili et al., 2007b, 2008; Malitsky et al., 2008).

To test whether the three *MYB*s play a role in controlling the spatial distribution of GLSs in Arabidopsis leaves, we dissected leaves of T-DNA knockout mutants and overexpression lines of *MYB28*, *MYB29*, or *MYB76* into three portions (vein, inner lamina, and edge) and measured GLS levels (Fig. 7; Supplemental Tables S12–S18). The data obtained in three independent experiments were pooled, since the ANOVA showed no significant difference between experiments. Generally, GLS chemotypes were as previously observed, except that *myb76-1* did not display a statistically significant decrease in 4msb in this experiment, even though it was still slightly lower in aliphatic GLSs than in the wild type (Supplemental Tables S12 and S13), and the chemotypes of the *MYB* overexpression lines were closer to that of the wild type in comparison with previous observations (Supplemental Tables S12 and S13). These differences are probably due to different growth conditions as compared with previous experiments (Sonderby et al., 2007). There was no difference in total leaf weights or weights of leaf parts among the genotypes (Supplemental Table S14), thereby allowing us to compare relative distributions of GLSs instead of absolute concentrations.

In wild-type Col-0 leaves, 52% of short-chained aliphatic GLSs was found in the leaf edge, with the rest being divided equally between the vein and inner

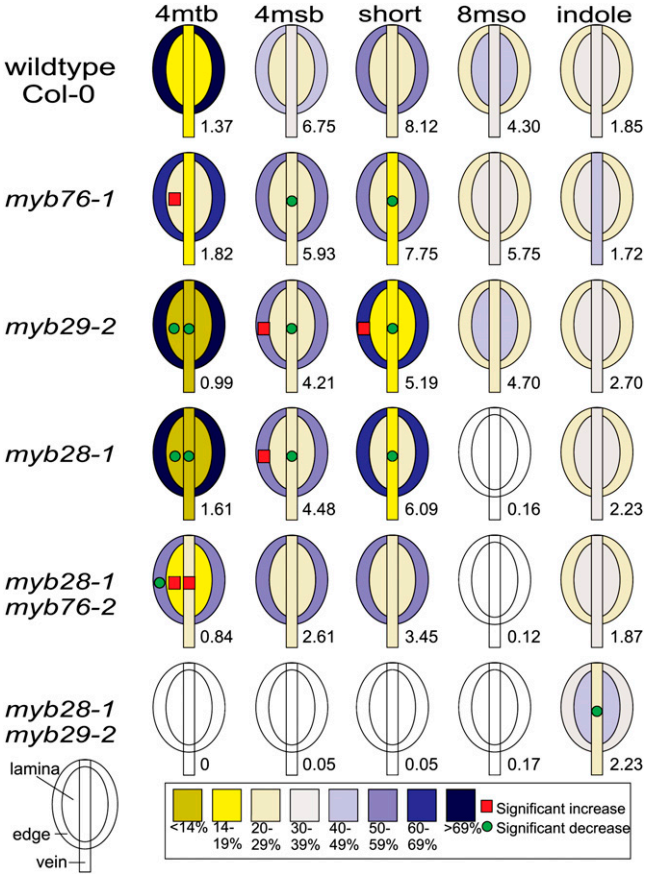

Figure 7. Distribution of GLSs in leaves of different *myb* knockouts. Leaf GLSs were analyzed in the edge, vein, and lamina from dissected leaves of wild-type Col-0 and various *myb* knockouts. The genotype is denoted on the left and the GLS (using the abbreviations in Supplemental Table S1) on top. The number to the right of each leaf corresponds to the total amount of GLS in nmol in the whole leaf. The colors denote proportions of a GLS in each leaf section in relation to total amount per leaf. Red squares and green circles indicate significant increases and decreases, respectively, in GLS distribution in comparison with the wild type. For exact relative distributions, see Supplemental Table S15. [See online article for color version of this figure.]

lamina (Fig. 7; Supplemental Tables S15 and S16). This distribution reflects that more than two-thirds of 4mtb and approximately half of 4msb accumulated in the edge (Fig. 7; Supplemental Table S15). The long-chained aliphatic GLS, 8mso, was more equally distributed throughout the leaf, with the highest portion in the lamina (Fig. 7; Supplemental Table S15). Conversely, 39% of indole GLSs were found in the vein, slightly less in the lamina, and the least in the edge (Fig. 7; Supplemental Table S15).

If the MYBs are controlling GLS distribution, then ectopic expression of the *MYB*s driven by the ubiquitously expressed 35S promoter would result in aliphatic GLSs being produced equally in the three leaf sections. As expected, an even distribution of total aliphatic GLS levels was observed across the sections

of the leaves overexpressing *MYB28*, *MYB29*, and *MYB76* (Sonderby et al., 2007; Supplemental Tables S17 and S18). This suggests that the spatial distribution of GLSs within the wild-type leaf is at least partially due to the spatial expression pattern of the *MYB*s.

In the *myb* knockout mutants, the relative distribution of short-chained aliphatic GLSs in the leaves was also changed (Fig. 7). For *myb28-1* and *myb29-2*, we observed decreased partitioning of all short-chained aliphatic GLSs in the vein and lamina, with elevated fractions in the margins. In contrast, for *myb76-1* and *myb28-1 myb76-2* mutants, decreased levels of 4mtb were observed in the margin but elevated levels were seen in the vein and lamina, suggesting that 4mtb is trapped in these tissues when *MYB76* is nonfunctional. Interestingly, 4msb in the *MYB76* mutants followed the trend to margin accumulation found in the *myb28-1* and *myb29-2* knockouts, which resulted in *myb76* having a distribution of short-chained aliphatic GLSs similar to wild-type Col-0. Our data suggest that the *MYB*s contribute to the determination of GLS distribution within the leaf and that *MYB76* may play a specific role in the distribution of 4mtb.

In spite of their effect on the distribution of short-chained aliphatic GLS distribution, none of the knockouts affected the distribution of the long-chained aliphatic GLS, 8mso (Fig. 7; Supplemental Table S15). This suggests a different regulation of the spatial distribution of long-chained aliphatic compared with short-chained aliphatic GLSs. As expected, distribution of indole GLSs in the leaf was not altered between wild-type Col-0 and any of the lines with altered levels of *MYB28*, *MYB29*, or *MYB76*, which corroborates the lack of impact of the three aliphatic *MYB*s on indole GLSs (Fig. 7; Supplemental Tables S15 and S17). The only exception to this observation was the *myb28-1 myb29-2* mutant, in which a slightly decreased proportion was present in the vein, which suggests that indole GLS distributions may be slightly affected when aliphatic GLS are heavily decreased.

DISCUSSION

Prior to this study, *MYB28*, *MYB29*, and *MYB76* were already firmly established as players in the regulation of aliphatic GLS biosynthesis (Gigolashvili et al., 2007b, 2008; Hirai et al., 2007; Sonderby et al., 2007; Beekwilder et al., 2008). Based on data from overexpression lines, clearly all three genes, *MYB28*, *MYB29*, and *MYB76*, were capable of inducing aliphatic GLSs, and they seemed to confer their regulation by positively regulating the transcription of aliphatic biosynthetic genes (Fig. 1A). Based on the chemotypes of the single knockouts, *MYB28* was regarded as the major important player in planta, *MYB29* as a lieutenant, and *MYB76* bearing an accessory role (Fig. 1B; Gigolashvili et al., 2009a). In this paper, we challenged the existing model, added significant information to the puzzle of the interaction between the genes (Fig. 8A), and suggest

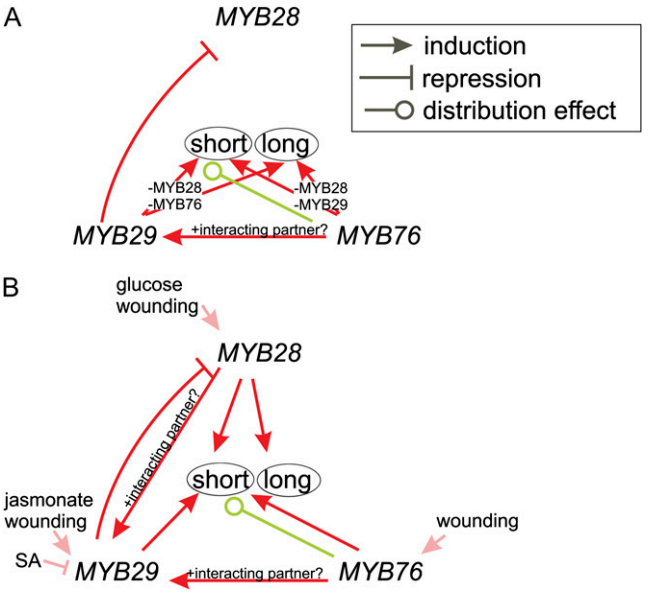

Figure 8. Models of aliphatic GLS regulation. A, Additions to the model of aliphatic GLS regulation depicted in Figure 1 by this paper. B, New predicted regulatory model in planta. Circles represent short- and long-chained aliphatic GLSs. Lines leading to circles indicate increasing (arrowheads) or spatial distribution in leaf (circles) effects on metabolites. Boxes indicate independence of the genes in the box for induction. Lines to genes represent induction (arrowheads) and repression (T-line), respectively, by another gene (red) or various treatments (pink). SA, Salicylic acid. [See online article for color version of this figure.]

an improved model for the role of *MYB28*, *MYB29*, and *MYB76* in the regulation of aliphatic biosynthesis in planta (Fig. 8B).

MYB76 Plays an Important Role in the Regulation of Transcription of Genes in Secondary Modifications and *MYB29*

Previously, *myb76* single T-DNA knockdowns were shown to have a small reduction in short-chained methylsulfinylalkyl-GLSs (Sonderby et al., 2007). In accordance with this chemotype (Fig. 3), the transcriptional analysis showed that transcription of FMO_{GSOX1}, responsible for the conversion of methylthioalkyl- to methylsulfinylalkyl-GLSs, was decreased in the *myb76* knockdowns (Fig. 6; Table II). However, the role of *MYB76* is not limited to FMO_{GSOX1}, as it also decreases transcripts of *AOP2*, another secondary modification enzyme, the core biosynthetic sulfotransferase *SOT17*, as well as *MYB29* (Table II). One might speculate that the effect of *MYB76* is purely performed through *MYB29*, but the apparent dependency is not absolute, since overexpression of *MYB76* in the almost aliphatic GLS-free *myb28 myb29* double knockout background induced significant production of aliphatic GLSs (Fig. 2; Supplemental Table S2), thereby showing independence of *MYB76* from *MYB28* and *MYB29* for the induction of aliphatic GLSs. This observation is consistent with the detectable induction of GLSs in the

myb28 myb29 double knockout when challenged with the lepidopteran insect *Mamestra brassicae* (Beekwilder et al., 2008) or under variable growth conditions (data not shown), which might be explained by induction of the normally lowly expressed *MYB76* (Sonderby et al., 2007; Gigolashvili et al., 2008).

Transactivation assays performed in cultured Arabidopsis cells left no doubt that *MYB76* can activate the promoters of both chain elongation and core biosynthetic enzymes, *MAM1*, *MAM3*, *CYP79F1*, *CYP79F2*, *CYP83A1*, and *SUR1* (Gigolashvili et al., 2008), whereas the capability of *MYB76* to activate the enzymes doing secondary modifications was not tested. Therefore, we can only speculate whether the specific effect on these genes is caused by a comparably higher binding affinity in comparison with aliphatic core biosynthetic enzymes in planta. Another proof for the role of *MYB76* in planta is added by the additive effect observed in the *myb28-1 myb76* double knockout on foliar aliphatic GLS levels (Fig. 3; Table I). This is in contrast with the epistatic effect observed in the *myb28 myb29* double knockout, which stresses that, even though *myb29* and *myb76* single knockout mutants have similar decreases in levels of short-chained aliphatic GLSs (Sonderby et al., 2007), *MYB29* has a more prominent role in upholding GLS accumulation. The only epistatic effect on single aliphatic GLSs observed in the *myb28-1 myb76* double knockout data set was on 4mtb, which agrees with a combined interaction of *MYB28* and *MYB76*, leading to an epistatic effect on the FMO_{GSOX}s. In addition, there is an epistatic effect of *MYB76* on total indole GLSs. The doubling of total indole GLSs in the *myb28-1* mutant (Fig. 3) is repressed in the *myb28-1 myb76* mutants, which indicates a possibly repressive effect of *MYB28* on indole GLSs but also that *MYB76* might be necessary for the induction of indole GLSs. Of the three aliphatic MYBs, only *MYB76* shows induction of *CYP79B2* in transactivation assay in Arabidopsis cells 2 to 3 d after induction (Gigolashvili et al., 2008). Further experiments are needed to explore a putative link of *MYB76* to indole GLS accumulation.

MYB76 does not play a role in seeds, since the aliphatic seed GLS level in *myb28-1 myb76* knockouts was not different from the *myb28-1* knockout (Table I). This agrees with a *MYB76* promoter-GUS analysis, in which *MYB76* expression was not found in siliques but only in inflorescences (Gigolashvili et al., 2008). In summary, we have shown a significant role for *MYB76* in determining GLS profile and leaf distribution.

Transcription of Biosynthetic Genes Does Not Reflect the Chemotype

The general view of positive regulators of metabolic pathways is that they act through the induction of biosynthetic transcripts and transporters, channeling intermediates between different compartments. However, in all the *myb* knockout mutants, there is a lack of correlation between total levels of biosynthetic transcripts and chemotypes. GLS biosynthetic transcripts are heavily down-regulated in the *myb28-1* single knockout (Fig. 6; Table II), which points to *MYB28* as the major transcriptional activator of aliphatic biosynthetic transcription in Arabidopsis (accession Col-0), as suggested previously (Gigolashvili et al., 2007b; Hirai et al., 2007). However, it remains a puzzle how *myb28-1* can retain as much as 73% of short-chained aliphatic GLSs in comparison with the wild type (Fig. 3), with its relatively low levels of biosynthetic transcripts (Table II).

Likewise, in spite of its almost GLS-free chemotype, biosynthetic transcripts in the *myb28-1 myb29-1* double knockout are remarkably close to the level measured in *myb28-1* (Fig. 6; Table II). Similarly, no change in biosynthetic transcripts was observed in the *myb29-2* mutant in comparison with the wild type (Table II; Fig. 6) in spite of its short-chained aliphatic GLS chemotype (Sonderby et al., 2007; Beekwilder et al., 2008; Gigolashvili et al., 2008). As such, the metabolic chemotype is uncoupled from the total level of biosynthetic transcripts, which could indicate that a decrease in one or a few biosynthetic transcripts is enough to change total aliphatic GLS accumulation. Alternatively, other mechanisms besides direct transcriptional regulation of aliphatic GLS biosynthesis are at play when determining aliphatic GLS accumulation.

The lack of effect on biosynthetic transcripts in the *myb29-2* mutant could indicate that it is not a positive regulator of biosynthetic transcripts. However, previous transactivation assays showed that *MYB29* alone activates transcription of the promoters of aliphatic biosynthetic genes in cultured Arabidopsis cells (Gigolashvili et al., 2007b, 2008). Together with the remaining short-chained foliar and seed aliphatic GLSs in the *myb28-1 myb76* double knockout, this supports a role for *MYB29* as a positive regulator of aliphatic biosynthetic transcripts. Therefore, the missing effect on transcripts in *myb29-2* is probably due to a concurrent increase in *MYB28* transcript (Table II; Fig. 6). However, since the *myb29* knockouts have altered chemotypes on short-chained aliphatic GLSs (Sonderby et al., 2007; Beekwilder et al., 2008; Gigolashvili et al., 2008), *MYB29* must affect other determinants for GLS accumulation besides the transcription of biosynthetic genes.

Changes in transcript levels related to sulfur assimilation were observed in the *myb29-2* mutant and the *myb28-1 myb29-1* double knockout (Supplemental Table S11). This may indicate that a concomitant decrease in aliphatic GLS biosynthetic transcripts and limitation in sulfur availability may be the cause of the uncoupling observed in the *myb28-1 myb29-1* knockout. Further studies are necessary to explain the uncoupling of aliphatic biosynthetic transcripts from GLS levels.

Interaction between the *MYB*s: *MYB29* as an Integration Point for Transcription?

The transcriptional data draw a picture of a highly interconnected network among the three *MYB*s. The

transcript of *MYB29* was significantly down-regulated and substantially decreased in the *myb76* and *myb28-1* knockouts, respectively (Table II), the latter supported by quantitative PCR data on a different *myb28* mutant (Beekwilder et al., 2008). Similarly, out of the three transcription factors, only *MYB29* was up-regulated in moderate overexpression lines of all three *MYB*s (Sonderby et al., 2007), which is further supported by independent data on overexpression lines in which *MYB76* was concurrently up-regulated (Gigolashvili et al., 2008). This seems to point toward a positive regulation by *MYB28* and *MYB76* on *MYB29*, which consequently plays an important role in the integration of signals from *MYB28* and *MYB76*. Possibly, *MYB29* constitutes a positive feed-forward loop in aliphatic GLS regulation similar to the indole GLS regulator, MYB122, which activates the other indole GLS regulator, *MYB51* (Gigolashvili et al., 2007a). Other examples of MYB feed-forward loops exist within anthocyanin biosynthesis, where the positive anthocyanin regulator *PRODUCTION OF ANTHOCYANIN PIGMENT1* feed forwards on *MYB114*, an R2R3 MYB transcription factor present in the same subclade (Dare et al., 2008). It might be a general feature of these small subclades of R2R3 MYB factors to primarily feed forward on one transcription factor that thus amplifies the signal from the other activators.

MYB29 cannot control indispensable regulatory functions, though, since the lack of *MYB29* only results in moderate decreases in aliphatic GLS levels (Sonderby et al., 2007; Beekwilder et al., 2008; Gigolashvili et al., 2008). The compensation of *MYB28* in the *myb29-2* mutant can be interpreted in two different ways: *MYB29* acts as a repressor of *MYB28* in wild-type Col-0, or alternatively, the plant may sense the decrease in aliphatic GLSs and subsequently act to compensate by up-regulating *MYB28*. This points to a possible feedback mechanism on *MYB28* by the lack of end products, which is a feature previously suggested by Mugford et al. (2009) and further supported by the up-regulation of *CYP79B2* in the absence of *CYP79B3* and visa versa (Celenza et al., 2005). Curiously, such a compensatory mechanism only feeds back on *MYB28* in the absence of *MYB29*, since neither *MYB76* nor *MYB29* is up-regulated in the GLS-lacking *myb28-1* knockout, nor is *MYB28* in the *myb76-1* knockdown. These data seem to indicate different signaling pathways for the activation of *MYB28*, *MYB29*, and *MYB76*.

The Presence of Unknown Interacting Partners

The in planta induction of *MYB29* by *MYB28* and *MYB76* (Table II; Beekwilder et al., 2008) is inconsistent with transactivation data performed in *Nicotiana benthamiana*, in which only *MYB76* could be induced by *MYB28*, *MYB29*, and *MYB76* whereas neither *MYB29* nor *MYB28* showed any transactivation (Gigolashvili et al., 2008). Possibly, *MYB28* and *MYB76* activate *MYB29* through another mechanism than direct transcriptional activation, maybe through the induction of an unknown transcription factor that subsequently induces *MYB29*. Alternatively, an unknown transcription factor, not present in *N. benthamiana*, interacts with MYB28 and MYB76 to facilitate the induction of *MYB29*. A common feature of R2R3 MYB transcription factors is the combinatorial control with bHLH and WD repeat proteins, as exemplified in the anthocyanin and proanthocyanidin biosynthesis (Davies and Schwinn, 2003). Recently, a bHLH transcription factor interacting with the indole GLS regulator *MYB51* was identified (T. Gigolashvili, personal communication), which suggests that a similar bHLH may interact with the aliphatic *MYB*s.

So far, the induction of long-chained aliphatic GLSs has largely been ascribed to the regulatory realm of *MYB28*, due to its long-chained aliphatic GLS chemotype in the *myb28* knockouts. However, trace amounts of long-chained aliphatic GLSs occasionally occur in both the *myb28-1* mutant (Hirai et al., 2007; Table I) and the *myb28-1 myb76* mutants (Table I), which indicates that under certain conditions at least *MYB29* can induce long-chained aliphatic GLSs in the absence of *MYB28*. Similarly, ectopic expression of *MYB29* and *MYB76* results in increased levels of long-chained aliphatic GLSs both in the absence (Figs. 2 and 4) and the presence of *MYB28* (Sonderby et al., 2007; Gigolashvili et al., 2008). Ectopic overexpression of *MYB28* in wild-type Col-0, on the other hand, did not result in increased long-chained aliphatic GLSs (Gigolashvili et al., 2007b; Sonderby et al., 2007). This speaks for the presence of an additional factor needed for the induction of long-chained aliphatic GLSs localized outside of the tissue where *MYB29* and *MYB76* are normally expressed and with which only these two MYBs can interact.

Roles of *MYB28*, *MYB29*, and *MYB76* in Leaf GLS Distribution

The primary accumulation sites for GLSs have been shown to be in the edge and midvein (Shroff et al., 2008), which is supported by our GLS distribution analysis. However, the accumulation in the edge is in contrast to the expression pattern of the regulatory proteins, which indicates that production takes place in the veins (Gigolashvili et al., 2007b, 2008; Malitsky et al., 2008). This suggests that the edge constitutes a "GLS sink" to which GLSs are transported from the veins (the source) through a yet unknown mechanism. Our analysis on the different *MYB* overexpression lines clearly showed that the putative source-sink relation between the veins and the edge is interrupted if the *MYB*s are ectopically expressed (Supplemental Tables S17 and S18). Thus, the specific spatial expression of the *MYB*s is at least partially responsible for the distribution of aliphatic GLSs in the leaf.

Since total GLS levels go down, the increase in the proportion of short-chained aliphatic GLSs in the leaf edge observed in the *myb28-1* and *myb29-2* knockouts is expected under the assumption of unchanged trans-

port processes (Fig. 7). However, the distribution of aliphatic GLSs in the *myb76-1* and *myb28-1 myb76-2* knockouts did not conform to this tendency. Instead, a smaller proportion of 4mtb is present in the edge in *myb76-1* and *myb28-1 myb76-2* in comparison with the wild type (Fig. 7; Supplemental Table S15). This cannot be explained solely by the presence of less GLSs, since the GLS levels in *myb76-1* under these growth conditions are similar to wild-type Col-0 (Fig. 7; Supplemental Table S12). Furthermore, given the small amount of 4msb in the *myb28-1 myb76-2* double knockout and presuming unchanged transport, one would expect a higher proportion of GLSs in the edge, as observed in the *myb28-1* and *myb29-2* knockouts. Additionally, since 4mtb follows the same pattern in the *myb28-1 myb76-2* double knockout as in the *myb76-1* single knockdown, this reveals a dominance of *MYB76* over *MYB28* in controlling spatial patterns. This indicates that *MYB76* changes the distribution of short-chained aliphatic GLSs from the vein to the edge in wild-type leaves, possibly by the regulation of a transporter. So far, no transporters of GLSs have been identified, even though several putative Suc transporters have been proposed to be involved in GLS transport (Nour-Eldin and Halkier, 2009). However, since the distribution of GLSs is still biased toward the leaf edge in the *myb76-1* and *myb28-1 myb76-2* knockouts, *MYB76* cannot be the only player in the regulation of distribution.

CONCLUSION

To our knowledge, this is the first comprehensive genome-wide transcriptional analysis of regulatory single knockout mutants of transcription factors all involved in the same metabolic pathway and without whose presence the metabolites of the corresponding pathway are not produced. This analysis showed that the level of biosynthetic transcripts was uncoupled from the levels of metabolites in the knockouts. This feature might hold true for other pathways as well and has implications for the way we view regulation of secondary metabolism. Our findings enabled us to decipher the individual roles of *MYB28*, *MYB29*, and *MYB76* and to identify new positive and negative cooperative interactions among these transcription factors that shape the aliphatic GLS profile. In combination with new insights about *MYB76* controlling the spatial distribution in the plant, this has led to an improved model for aliphatic GLS regulation (Fig. 8B). The next step in the field will be to identify putative interaction partners of the MYBs to explain their complex interactions and to find what regulates the regulators.

MATERIALS AND METHODS

Plant Cultivation

Arabidopsis (*Arabidopsis thaliana* accession Col-0) transgenics and mutants in Pindstrup 2 sphagnum medium (Pindstrup Mosebrug) were grown in a growth chamber (HEMZ 20/240/S; Thermo Heraeus) with 100 μE light intensity, 16/8-h light/dark cycle, 20°C, and 70% relative humidity.

T-DNA Insertion Mutants and Creation of Overexpression Lines

T-DNA insertion mutants in *At5g61420* (line SALK_136312 = *myb28-1*), *At5g07690* (lines GABI_868E02 = *myb29-1* and SM.34316 = *myb29-2*), and *At5g07700* (lines SALK_096949 = *myb76-1* and SALK_055242 = *myb76-2*) have been described previously (Sonderby et al., 2007). To construct the double mutants *myb28-1 myb76-1*, *myb28-1 myb76-2*, and *myb28-1 myb29-2*, the respective homozygous single knockouts were crossed with each other. The F1 plants were self-fertilized, and progeny in the F2 generation were genotyped (Sonderby et al., 2007). Each line originally came from a segregating heterozygous individual that, after crossing, was allowed to self, thereby allowing unlinked polymorphisms to segregate away.

The generation of the *35S:MYB29* and *35S:MYB76* overexpression constructs has been described previously (Sonderby et al., 2007). Binary plasmids were transferred to *Agrobacterium tumefaciens* strain C58 (Zambryski et al., 1983) and transformed into Arabidopsis plants (*myb28-1 myb76-1*, *myb28-1 myb76-2*, and *myb28-1 myb29-1* double knockouts) according to the floral dip method (Clough and Bent, 1998). Transgenic T1 plants were selected on half-strength Murashige and Skoog medium with 50 mg L^{-1} kanamycin.

GLS Extraction and Analysis

GLS extraction was performed as described previously (Sonderby et al., 2007). For analysis of leaves, 30 to 70 mg of leaves was harvested just before bolting (22–25 d after germination). For analysis of seeds, 10 seeds were used for the extraction. HPLC analysis was performed as described previously (Hansen et al., 2007).

GLS Statistical Analysis

GLS contents were analyzed via ANOVA utilizing SAS proc glm. All comparisons contained multiple independent experiments that were tested for significance as a fixed effect to allow for testing an interaction with genotype. For *MYB76*, there were two independent T-DNA mutant lines. Both lines were assayed, and the difference between the independent mutants was tested as a nested factor using the factor MYB76 (line). This allowed us to test if the effects on GLS accumulation were due to the presence of any T-DNA within *MYB76* (line) or if there was a difference between the separate T-DNA alleles. Sums of squares, *F* values, and *P* values are presented. More details on specific models and sample numbers can be found in the tables of the individual experiments.

Dissection Experiment

Wild-type Col-0, transgenic lines, and T-DNA mutants (see above) were grown in Pindstrup 2 sphagnum medium (Pindstrup Mosebrug) in a growth chamber (HEMZ 20/240/S; Thermo Heraeus) with 100 μE light intensity, 8/16-h light/dark cycle, 17°C to 20°C, and 70% relative humidity. At 6 to 7 weeks after germination, two leaves including the entire petiole were cut from each plant. One leaf was immediately submerged in 300 μL of 85% (v/v) methanol containing 0.02 mM sinigrin as internal standard. The other leaf was dissected with a scalpel with two cuts 1 mm on either side of the midvein and three cuts along the edges, about 1 mm from each edge, according to the drawings in Figure 7. Each section was weighed and immediately submerged in 300 μL of 85% methanol supplemented with 0.02 mM sinigrin. Four replicates were made per genotype. GLSs were extracted and measured as described previously (Sonderby et al., 2007). The experiment was repeated three times.

Dissection Statistical Analysis

To compare GLS partitioning among individual genotypes, we added up total GLS amounts in each dissected leaf and calculated the percentage of each individual GLS in each separate section. The three sections were then utilized as three variables within a single section factor in the ANOVA. Three independently replicated experiments for the dissection experiment each with four plants per genotype were done. Experiment × experiment and genotype × experiment interactions were included in the original model, but

as the genotype × experiment term showed no significance, it was dropped from the final model. To test if GLSs are lost in the dissection, we individually summed up all GLSs in the dissected sections and statistically compared the levels of dissected and undissected leaves. No difference was observed in GLS levels between the dissected and intact leaves as tested by ANOVA (data not shown). This was done for all genotypes. As such, we combined all leaves to calculate the average total GLS level in a single leaf from each genotype.

Microarray Analysis of *MYB* Knockouts

Plants for the various genotypes were grown as described previously (Sonderby et al., 2007). At 25 d post germination, a fully expanded mature leaf was harvested, weighed, and analyzed for total aliphatic GLS content via HPLC. The remaining plant material was collected and flash frozen, and total RNA was extracted via RNeasy columns (Qiagen). Two independent plants were combined to provide sufficient starting material for a single RNA extraction. Two independent samples were obtained per mutant, thus providing 4-fold replication. Eight wild-type Col-0 RNA samples were obtained. This provided a total of 32 independent microarrays. Labeled copy RNA was prepared and hybridized, according to the manufacturer's guidelines (Affymetrix), to whole genome Affymetrix ATH1 GeneChip microarrays, containing 22,746 Arabidopsis transcripts. The GeneChips were scanned with an Affymetrix GeneArray 2500 Scanner, and data were acquired via the Microarray Suite software MAS 5.0 at the Functional Genomics Laboratory (University of California, Berkeley). Robust Multichip Average normalization was used to obtain gene expression levels for all data analyses (Irizarry et al., 2003).

Microarray Statistical Analysis

The gene expression data were analyzed via individual gene ANOVA for each transcript. This was done by conducting ANOVA on each gene using the independent samples for both mutants and the wild type. The ANOVA calculations were programmed into Microsoft Excel to obtain all appropriate sums of squares and the *F* values for the effect of the genotype (wild type versus mutant) and replicate effects for each transcript. The *P* values for genotype (wild type versus mutant) are presented after a FDR adjustment to the 0.05 level (Supplemental Table S10; Benjamini and Hochberg, 1995). For downstream analysis, biosynthetic pathways were obtained from AraCyc version 3.4 (http://www.arabidopsis.org/biocyc/) and modified to better organize the pathways based on metabolites of importance for GLS synthesis (Supplemental Table S10).

Supplemental Data

The following materials are available in the online version of this article.

Supplemental Table S1. GLS abbreviations and chemical structures.

Supplemental Table S2. Foliar GLSs in *35S:MYB76* into *myb28-1 myb29-1* double knockout and *35S:MYB29* into *myb28-1 myb76* double knockout, T1 plants.

Supplemental Table S3. ANOVAs comparing T1 leaf GLSs between wild-type Col-0, *MYB* knockouts, and *35S:MYB76* in *myb28-1 myb29-1* double knockout and *35S:MYB29* in *myb28-1 myb76* double knockout.

Supplemental Table S4. Seed GLSs in *35S:MYB76* into *myb28-1 myb29-1* double knockout and *35S:MYB29* into *myb28-1 myb76* double knockouts, T2 seeds.

Supplemental Table S5. ANOVAs comparing T2 seed GLSs between wild-type Col-0, *MYB* knockouts, and *35S:MYB76* in *myb28-1 myb29-1* double knockout and *35S:MYB29* in *myb28-1 myb76* double knockout.

Supplemental Table S6. ANOVAs for leaf GLSs in wild-type Col-0, *myb76*, *myb28-1*, and *myb28-1 myb76* knockouts.

Supplemental Table S7. Foliar GLSs in wild-type Col-0, *myb28-1*, *myb76*, and *myb28-1 myb76* T-DNA knockouts.

Supplemental Table S8. ANOVAs for seed GLSs in wild-type Col-0, *myb76*, *myb28-1*, and *myb28-1 myb76* knockouts.

Supplemental Table S9. GLS gene microarray analysis comparing Col-0 versus various *MYB* loss-of-function knockouts.

Supplemental Table S10. Individual gene microarray analysis comparing Col-0 versus MYB knockouts.

Supplemental Table S11. Microarray data, selected transcripts, and sulfur utilization biosynthetic pathways.

Supplemental Table S12. GLS levels in whole leaf and sum of dissection portions.

Supplemental Table S13. ANOVAs for leaf GLSs in whole leaf and sum of dissection portions.

Supplemental Table S14. Weight parameters.

Supplemental Table S15. Fractions of GLSs in dissected leaves of *MYB* knockouts.

Supplemental Table S16. ANOVAs for fractions of GLSs in dissected leaves of *MYB* knockouts.

Supplemental Table S17. Fractions of GLSs in dissected leaves of plants overexpressing *MYB* transcription factors.

Supplemental Table S18. ANOVAs for proportions of GLSs in dissected leaves of plants overexpressing *MYB* transcription factors.

Received October 12, 2009; accepted March 23, 2010; published March 26, 2010.

LITERATURE CITED

Andreasson E, Bolt JL, Hoglund AS, Rask L, Meijer J (2001) Different myrosinase and idioblast distribution in Arabidopsis and *Brassica napus*. Plant Physiol **127:** 1750–1763

Bednarek P, Pislewska-Bednarek M, Svatos A, Schneider B, Doubsky J, Mansurova M, Humphry M, Consonni C, Panstruga R, Sanchez-Vallet A, et al (2009) A glucosinolate metabolism pathway in living plant cells mediates broad-spectrum antifungal defense. Science **323:** 101–106

Beekwilder J, van Leeuwen W, van Dam NM, Bertossi M, Grandi V, Mizzi L, Soloviev M, Szabados L, Molthoff JW, Schipper B, et al (2008) The impact of the absence of aliphatic glucosinolates on insect herbivory in Arabidopsis. PLoS One **3:** e2068

Benjamini Y, Hochberg Y (1995) Controlling the false discovery rate: a practical and powerful approach to multiple testing. J R Stat Soc B **57:** 289–300

Brown PD, Tokuhisa JG, Reichelt M, Gershenzon J (2003) Variation of glucosinolate accumulation among different organs and developmental stages of Arabidopsis thaliana. Phytochemistry **62:** 471–481

Celenza JL, Quiel JA, Smolen GA, Merrikh H, Silvestro AR, Normanly J, Bender J (2005) The Arabidopsis ATR1 Myb transcription factor controls indolic glucosinolate homeostasis. Plant Physiol **137:** 253–262

Chen S, Glawischnig E, Jorgensen K, Naur P, Jorgensen B, Olsen CE, Hansen CH, Rasmussen H, Pickett JA, Halkier BA (2003) CYP79F1 and CYP79F2 have distinct functions in the biosynthesis of aliphatic glucosinolates in Arabidopsis. Plant J **33:** 923–937

Clough SJ, Bent AF (1998) Floral dip: a simplified method for Agrobacterium-mediated transformation of Arabidopsis thaliana. Plant J **16:** 735–743

Dare AP, Schaffer RJ, Lin-Wang K, Allan AC, Hellens RP (2008) Identification of a cis-regulatory element by transient analysis of co-ordinately regulated genes. Plant Methods **4:** 17

Davies KM, Schwinn KE (2003) Transcriptional regulation of secondary metabolism. Funct Plant Biol **30:** 913–925

Dixon RA, Strack D (2003) Phytochemistry meets genome analysis, and beyond. Phytochemistry **62:** 815–816

Falk KL, Tokuhisa JG, Gershenzon J (2007) The effect of sulfur nutrition on plant glucosinolate content: physiology and molecular mechanisms. Plant Biol (Stuttg) **9:** 573–581

Gigolashvili T, Berger B, Flugge UI (2009a) Specific and coordinated control of indolic and aliphatic glucosinolate biosynthesis by R2R3-MYB transcription factors in Arabidopsis thaliana. Phytochem Rev **8:** 3–13

Gigolashvili T, Berger B, Mock HP, Muller C, Weisshaar B, Flugge UI (2007a) The transcription factor HIG1/MYB51 regulates indolic glucosinolate biosynthesis in Arabidopsis thaliana. Plant J **50:** 886–901

Gigolashvili T, Engqvist M, Yatusevich R, Muller C, Flugge UI (2008) HAG2/MYB76 and HAG3/MYB29 exert a specific and coordinated

control on the regulation of aliphatic glucosinolate biosynthesis in Arabidopsis thaliana. New Phytol **177:** 627–642

Gigolashvili T, Yatusevich R, Berger B, Muller C, Flugge UI (2007b) The R2R3-MYB transcription factor HAG1/MYB28 is a regulator of methionine-derived glucosinolate biosynthesis in Arabidopsis thaliana. Plant J **51:** 247–261

Gigolashvili T, Yatusevich R, Rollwitz I, Humphry M, Gershenzon J, Flugge UI (2009b) The plastidic bile acid transporter 5 is required for the biosynthesis of methionine-derived glucosinolates in *Arabidopsis thaliana*. Plant Cell **21:** 1813–1829

Grotewold E (2008) Transcription factors for predictive plant metabolic engineering: are we there yet? Curr Opin Biotechnol **19:** 138–144

Grubb CD, Abel S (2006) Glucosinolate metabolism and its control. Trends Plant Sci **11:** 89–100

Grubb CD, Zipp BJ, Ludwig-Muller J, Masuno MN, Molinski TF, Abel S (2004) Arabidopsis glucosyltransferase UGT74B1 functions in glucosinolate biosynthesis and auxin homeostasis. Plant J **40:** 893–908

Halkier BA, Gershenzon J (2006) Biology and biochemistry of glucosinolates. Annu Rev Plant Biol **57:** 303–333

Hansen BG, Kliebenstein DJ, Halkier BA (2007) Identification of a flavin-monooxygenase as the S-oxygenating enzyme in aliphatic glucosinolate biosynthesis in Arabidopsis. Plant J **50:** 902–910

Hirai MY, Klein M, Fujikawa Y, Yano M, Goodenowe DB, Yamazaki Y, Kanaya S, Nakamura Y, Kitayama M, Suzuki H, et al (2005) Elucidation of gene-to-gene and metabolite-to-gene networks in Arabidopsis by integration of metabolomics and transcriptomics. J Biol Chem **280:** 25590–25595

Hirai MY, Sugiyama K, Sawada Y, Tohge T, Obayashi T, Suzuki A, Araki R, Sakurai N, Suzuki H, Aoki K, et al (2007) Omics-based identification of Arabidopsis Myb transcription factors regulating aliphatic glucosinolate biosynthesis. Proc Natl Acad Sci USA **104:** 6478–6483

Irizarry RA, Hobbs B, Collin F, Beazer-Barclay YD, Antonellis KJ, Scherf U, Speed TP (2003) Exploration, normalization, and summaries of high density oligonucleotide array probe level data. Biostatistics **4:** 249–264

Juge N, Mithen RF, Traka M (2007) Molecular basis for chemoprevention by sulforaphane: a comprehensive review. Cell Mol Life Sci **64:** 1105–1127

Kliebenstein DJ, Kroymann J, Brown P, Figuth A, Pedersen D, Gershenzon J, Mitchell-Olds T (2001a) Genetic control of natural variation in Arabidopsis glucosinolate accumulation. Plant Physiol **126:** 811–825

Kliebenstein DJ, Lambrix VM, Reichelt M, Gershenzon J, Mitchell-Olds T (2001b) Gene duplication in the diversification of secondary metabolism: tandem 2-oxoglutarate-dependent dioxygenases control glucosinolate biosynthesis in *Arabidopsis*. Plant Cell **13:** 681–693

Levy M, Wang Q, Kaspi R, Parrella MP, Abel S (2005) Arabidopsis IQD1, a novel calmodulin-binding nuclear protein, stimulates glucosinolate accumulation and plant defense. Plant J **43:** 79–96

Li J, Hansen BG, Ober JA, Kliebenstein DJ, Halkier BA (2008) Subclade of flavin-monooxygenases involved in aliphatic glucosinolate biosynthesis. Plant Physiol **148:** 1721–1733

Malitsky S, Blum E, Less H, Venger I, Elbaz M, Morin S, Eshed Y, Aharoni A (2008) The transcript and metabolite networks affected by the two clades of Arabidopsis glucosinolate biosynthesis regulators. Plant Physiol **148:** 2021–2049

Maruyama-Nakashita A, Nakamura Y, Tohge T, Saito K, Takahashi H (2006) Arabidopsis SLIM1 is a central transcriptional regulator of plant sulfur response and metabolism. Plant Cell **18:** 3235–3251

Mewis I, Tokuhisa JG, Schultz JC, Appel HM, Ulrichs C, Gershenzon J (2006) Gene expression and glucosinolate accumulation in Arabidopsis thaliana in response to generalist and specialist herbivores of different feeding guilds and the role of defense signaling pathways. Phytochemistry **67:** 2450–2462

Mugford SG, Yoshimoto N, Reichelt M, Wirtz M, Hill L, Mugford ST, Nakazato Y, Noji M, Takahashi H, Kramell R, et al (2009) Disruption of adenosine-5′-phosphosulfate kinase in *Arabidopsis* reduces levels of sulfated secondary metabolites. Plant Cell **21:** 910–927

Nour-Eldin H, Halkier BA (2009) Piecing together the transport pathway of aliphatic glucosinolates. Phytochem Rev **8:** 53–67

Quattrochio F, Baudry A, Lepiniec L, Grotewold E (2006) The regulation of flavonoid biosynthesis. *In* E Grotewold, ed, The Science of Flavonoids. Springer, New York, pp 97–122

Reintanz B, Lehnen M, Reichelt M, Gershenzon J, Kowalczyk M, Sandberg G, Godde M, Uhl R, Palme K (2001) Bus, a bushy *Arabidopsis* CYP79F1 knockout mutant with abolished synthesis of short-chain aliphatic glucosinolates. Plant Cell **13:** 351–367

Sawada Y, Toyooka K, Kuwahara A, Sakata A, Nagano M, Saito K, Hirai MY (2009) Arabidopsis bile acid:sodium symporter family protein 5 is involved in methionine-derived glucosinolate biosynthesis. Plant Cell Physiol **50:** 1579–1586

Schuster J, Binder S (2005) The mitochondrial branched-chain aminotransferase (AtBCAT-1) is capable to initiate degradation of leucine, isoleucine and valine in almost all tissues in Arabidopsis thaliana. Plant Mol Biol **57:** 241–254

Shroff R, Vergara F, Muck A, Svatos A, Gershenzon J (2008) Nonuniform distribution of glucosinolates in Arabidopsis thaliana leaves has important consequences for plant defense. Proc Natl Acad Sci USA **105:** 6196–6201

Sonderby IE, Hansen BG, Bjarnholt N, Ticconi C, Halkier BA, Kliebenstein DJ (2007) A systems biology approach identifies a R2R3 MYB gene subfamily with distinct and overlapping functions in regulation of aliphatic glucosinolates. PLoS One **2:** e1322

Stracke R, Ishihara H, Huep G, Barsch A, Mehrtens F, Niehaus K, Weisshaar B (2007) Differential regulation of closely related R2R3-MYB transcription factors controls flavonol accumulation in different parts of the Arabidopsis thaliana seedling. Plant J **50:** 660–677

Traka M, Mithen R (2009) Glucosinolates, isothiocyanates and human health. Phytochem Rev **8:** 269–282

Wentzell AM, Rowe HC, Hansen BG, Ticconi C, Halkier BA, Kliebenstein DJ (2007) Linking metabolic QTLs with network and cis-eQTLs controlling biosynthetic pathways. PLoS Genet **3:** 1687–1701

Zambryski P, Joos H, Genetello C, Leemans J, Montagu MV, Schell J (1983) Ti plasmid vector for the introduction of DNA into plant cells without alteration of their normal regeneration capacity. EMBO J **2:** 2143–2150

Zhao Z, Zhang W, Stanley BA, Assmann SM (2008) Functional proteomics of *Arabidopsis thaliana* guard cells uncovers new stomatal signaling pathways. Plant Cell **20:** 3210–3226